

Negative Poisson's ratio polyethylene foams

B. BRANDEL, R. S. LAKES^{*,‡,§,¶}

*Materials Science Program, *Department of Engineering Physics, ‡Engineering Mechanics Program, §Biomedical Engineering Department, ¶Rheology Research Center, University of Wisconsin-Madison, 147 Engineering Research Building, 1500 Engineering Drive, Madison, WI 53706-1687, USA*
E-mail: lakes@engr.wisc.edu

Various polyethylene foams were subjected to thermo-mechanical processing with the aim of transforming them into re-entrant materials exhibiting negative Poisson's ratio. Following transformation, large cell foams (cell sizes of 1 and 2 mm) exhibited re-entrant cell structure and negative Poisson's ratio over a range of processing times and temperatures. Poisson's ratio vs. strain for these foams was similar to prior results for reticulated polyurethane foams. Following processing, microcellular polyethylene foam was densified but cells remained convex; it did not exhibit a substantial negative Poisson's ratio. This foam had a different transition temperature as determined via DSC than the large cell foams. © 2001 Kluwer Academic Publishers

1. Introduction

1.1. Polymeric foams

Polymeric foams are widely used in such applications as seat cushions, floats, coffee cups, sign overlays, and packaging materials. Foams are used for a variety of reasons including insulation, weight reduction, buoyancy, energy dissipation, and stress redistribution. It is possible to make a foam from most materials [1]. Microcellular foams are a relatively new development [2] with the original intent of reducing the amount of material required in manufacturing. These foams may have cell diameters as small as 10 μm . As with other polymers and polymer foams, they are viscoelastic [3]. Microcellular structure is produced [4, 5] by first saturating the polymer sample with a non-reactive gas, typically CO_2 or N_2 , in a high pressure environment, then reducing the ambient pressure to promote nucleation and growth of microcells. Neither strength nor stiffness of foam depends on cell size alone [6]. However, some foam properties are improved [7] by creating a microcellular structure, possibly as a result of changes in the solid phase. Polyethylene foams, most commonly closed cell, is available in a range of densities for packing and cushioning applications and for sports equipment. Polyethylene foams are also used in pads to prevent injury in falls [8] and to reduce pressure upon ulcers [9].

1.2. Poisson's ratio

Poisson's ratio ν , is defined as the negative of transverse strain divided by the axial strain. In isotropic materials, the Poisson's ratio must lie between -1 and $+0.5$ [10] following stability arguments. This range of Poisson's ratio corresponds to positive shear and bulk moduli. If

either modulus were to be negative, an unconstrained block of material would be unstable to small perturbation. Until recently, the range of Poisson's ratio for isotropic materials was thought to be between 0 and $+0.5$. The majority of materials have a Poisson's ratio close to $1/3$, although rubbery materials have values approaching $1/2$. Isotropic foam materials exhibiting negative Poisson's ratio behaviour were first produced by Lakes [11]. Such materials have been referred to as anti-rubber [12], auxetic [13], and dilational [14]. The principle behind creating negative Poisson's ratio foam is that of a re-entrant structure. The convex cells of a normal foam are converted by permanent triaxial compression into a re-entrant form with buckled ribs. The re-entrant cells unfold under tension giving rise to the negative Poisson's ratio. As a result these foams have unusual mechanical properties. For example consider the relationship between Young's Modulus, E , and the modulus of rigidity, G , $E = 2G(1 + \nu)$. In normal isotropic materials, the elastic modulus is at least twice G . However, when the Poisson's ratio is less than zero, the two moduli begin to come closer until, at $\nu = -0.5$, they are equal. Beyond $\nu = -0.5$, the modulus of rigidity actually exceeds the elastic modulus [15]. The negative Poisson's ratio enables these materials to function as unusual press-fit fasteners, to conform by bending to convex surfaces, and to enhance the performance of piezoelectric transducers. Foams with a negative Poisson's ratio also have enhanced properties such as tear resistance and the ability to cushion objects upon impact without bottoming.

Each kind of foam has a unique set of processing parameters which give rise to a negative Poisson's ratio. The goal of this research is to study the transformation of polyethylene foams of several cell sizes.

2. Materials and methods

2.1. Specimens and processing

Three kinds of foam were examined, a blue, large cell polyethylene (Sentinel, CELLECT LLC, Hyannis, MA 02601), a cross-linked, open cell polyolefin foam with a cell size of about 2 mm and a density of 29 kg/m^3 , a white, large cell polyethylene (Sentinel, CELLECT LLC, Hyannis, MA 02601), a cross-linked, open cell polyolefin foam with a cell size of 1 mm and a density of 26 kg/m^3 , and a microcellular polyethylene (Sentinel, CELLECT LLC, Hyannis, MA 02601), a cross-linked, closed cell polyolefin with a cell size of 0.1 mm [16] and a density of 37 kg/m^3 . Samples were cut from the bulk foam using a hot wire saw. The saw consists of 28 gauge steel wire held between two adjustable clamps. The wire was aligned using a carpenter's square and heated with a current of three amps from a DC power supply. The microcellular polyethylene may also be cut easily with a hacksaw because of its comparatively high stiffness by drawing the blade repeatedly in one direction.

Initial sample size was determined based upon the desired volumetric compression ratio during transformation. Examination of the relationship between the compression ratio and the Poisson's ratio was examined by Choi and Lakes [15]. In addition, spring back, or recovery must also be considered when determining the initial sample size for a desired final compression ratio. Spring back is the difference in the desired final volume of the sample (usually the mold volume) and the true final volume of the sample. A desired compression ratio of 2 to 2.4 was used. This was a compromise between several factors including the limited size of some foam slabs and the comparative stiffness of the microcellular material, which made it difficult to insert large pieces into a mold. Previous studies [15] on reticulated polyurethane foam showed the optimal volumetric compression ratio to be about 3.5 in order to achieve the most negative value of Poisson's ratio, $\nu = -0.7$; a compression ratio of 2 sufficed to achieve $\nu = -0.3$.

The microcellular polyethylene samples were cut to dimensions of approximately $2.7 \text{ cm} \times 2.7 \text{ cm} \times 6.0 \text{ cm}$ giving an initial compression ratio of approximately 2. Sample sizes for the large cell polyethylene were about $3.0 \text{ cm} \times 3.0 \text{ cm} \times 6.3 \text{ cm}$, which gives an initial compression ratio of approximately 2.4. Specimens were placed in molds of interior dimensions $2.2 \text{ cm} \times 2.2 \text{ cm} \times 12.8 \text{ cm}$. Tubular spacers were used to govern the final specimen length. Flat aluminum plates slightly smaller than the cross section of the tube and 0.2 cm thick with 16 holes 1 mm in diameter were placed between spacers and foam to distribute stress and allow escape of compressed air. The assembly of specimen, spacers, and mold were held by a clamp.

Specimens were subjected to thermal treatment [11], at various times and temperatures. Each sample was removed from the furnace, taken out of the mold immediately, and cooled at room temperature in air. The optimal processing parameters are determined empirically. If time and temperature are insufficient, the foam

acquires no permanent deformation and returns to its original size after removal from the mold. If time and temperature are excessive, the foam ribs adhere to each other or the foam adheres to the mold.

Due to the comparatively greater stiffness of the microcellular polyethylene foam, initial Poisson's ratio screening tests become more complex than those for the large cell polyethylene and the polyurethane foams examined previously [15]. In the case of the more compliant foams, a simple stretching or compression of the foams usually reveals the sign of the Poisson's ratio of the material to the unaided eye. This cannot be done with the stiffer microcellular material; a full characterization is required. Anisotropy was measured in the microcellular foams in independent tests with a screw driven test machine.

Some microcellular samples were rolled to determine if they could be converted from closed cell to open cell structure. Powered steel rollers with controlled gap from 12.5 mm to 1.9 mm were used. Other microcellular samples were subjected to vacuum less than 2×10^{-5} torr for 80 minutes.

2.2. Compression ratio measurement

The sample dimensions were measured and recorded both before and after processing. The compression ratio and spring back were determined by using the sample's initial volume (V_i), the sample's final volume (V_f), and the volume of the mold (V_m). The initial compression ratio (CR_i) is V_i/V_m . The final compression ratio (CR_f) is V_i/V_f .

2.3. SEM imaging, DSC measurement and solubility procedure

For SEM study, samples were coated with gold using a Denton Vacuum Desk II sputter machine. During sputtering, the chamber was pumped down below 50 mTorr and then sputtered using a gold target in argon at a pressure of approximately 75 mTorr. The sample plug was then inserted into the Jeol JSM-6100 scanning electron microscope for examination.

The DSC used was a Perkin-Elmer DSC7 Differential Scanning Calorimeter using Pyris software. A baseline consisting of an empty sample holder identical to the ones used for the foam samples was run through the same heating and cooling cycles as the foam samples. This baseline was then subtracted from the results obtained in the foam runs to produce the final graph. The foams were subjected to a cooling and heating rate of $20^\circ\text{C}/\text{min}$. Three complete heating and cooling runs of both foams were performed on each sample and an average was calculated.

To test solubility, foam samples were refluxed in xylene and decahydronaphthalene for 3 hours.

2.4. Thermal conductivity

The thermal response time of the foams was determined as follows. A temperature probe with a National Semiconductor LM 355 temperature diode with an

output of 10 mV/K was inserted into a sample and heated to 70°C. Once equilibrium was established, the sample was removed from the furnace and allowed to cool in air supported by the probe. The voltage from the temperature diode was recorded as a function of time using a digital oscilloscope.

2.5. Poisson's ratio measurement

The laser method used for measurement was based on the approach of Kugler *et al.* [17] for measurement of Poisson's ratios of rubbery materials. The method is capable of the considerable precision required to measure Poisson's ratios on the order of 0.499. Due to the heterogeneous nature of the foams in the present study, such a high level of precision cannot be obtained even with perfect execution. Even so, the laser method is superior to pointwise methods since some of the heterogeneous deformation field [18] is averaged over. Several pointwise methods such as a fiber optic displacement probe were used in initial trials, but results were noisy since the motion of an individual cell is not necessarily representative of the foam as a whole.

The laser method uses a measurement of the change in the amount of light passing by a sample in order to determine the change in its width due to the Poisson effect. The light source was a Melles Griot HeNe laser of 5 mW nominal power. The beam was diverged by a beam spreader lens. Opaque shields were used to control the size and shape of the light beam. Transmitted power was measured with a Newport Model 835 optical power meter. A light baffle in front of the detector served to minimize the effects of background lighting. The set-up (Fig. 1) was mounted on a Newport honeycomb optical table top.

The system was calibrated using a movable shield attached to a micrometer screw. This shield was moved a specific distance, and the change in the light detected was recorded as a function of known shield position. The calibration curve was then curve fitted with a quadratic. The slope of each calibration curve was determined by taking the derivative of each curve fit equation. Because the beam power was not spatially uniform the sample's initial position along the curve was determined in order to obtain the relationship between beam power and transverse movement of the sample edge.

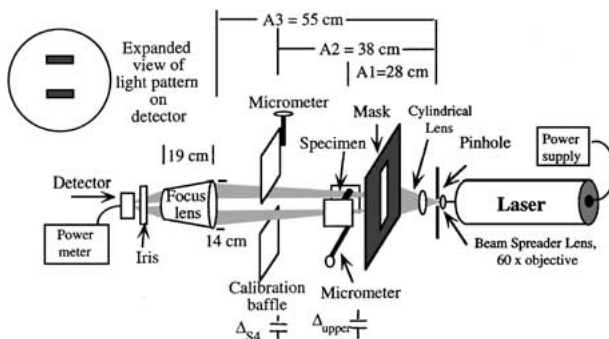


Figure 1 Diagram of the laser system for measuring Poisson's ratio, showing the light beam in relation to the sample and the calibration shield. The scale of this diagram is exaggerated to show the angular relationships. Also shown are parameters used in the calculations.

Gauge marks were first drawn on the sample approximately two centimeters apart along the transverse direction. The sample was placed between the laser and the detector between two blocks. One of the blocks is movable and is controlled by a micrometer screw. This screw was turned until the sample was suspended using the minimal amount of force. The gauge length was measured using a caliper and recorded. The amount of background light was also recorded by blocking the laser light and recording the reading on the power meter. Background light was reduced by adding a variable iris aperture directly in front of the power meter. The aperture was adjusted until it was slightly wider than the strips of light used for measurement. There was about 0.4 microwatts background light, compared with 100 to 200 microwatts of signal light. The sample was strained the desired amount via a micrometer screw. During sample deformation, the Poisson effect causes the specimen lateral surfaces to either constrict or expand. This movement causes the strips of light projected on the detector to become wider or narrower in proportion to the amount of change in the foam's transverse dimension. This results in a change of the light intensity detected.

An argument of similar triangles was used to infer the transverse displacement required for calculation of Poisson's ratio from the intensity of light received by the detector. Since the sample was positioned such that the amount of light detected above the sample was roughly equal to the light below the sample the light in each split segment of the shadowed beam was about the same.

All tests over a range of strain were done by straining the sample without removing it from the set-up. The sample was strained, the power readings were taken five seconds after the strain was completed, and the sample was strained to the next desired level one minute after the previous strain was started. To examine the strain dependence of Poisson's ratio in tension, samples were cemented with contact adhesive to acrylic flanges approximately 5 cm long and 2.5 cm wide and 0.2 cm thick. The flanges were fastened to optical mounts.

To evaluate viscoelastic effects, lateral deformation was monitored as a function of time following an abrupt compressive strain.

3. Results and discussion

3.1. Microstructure

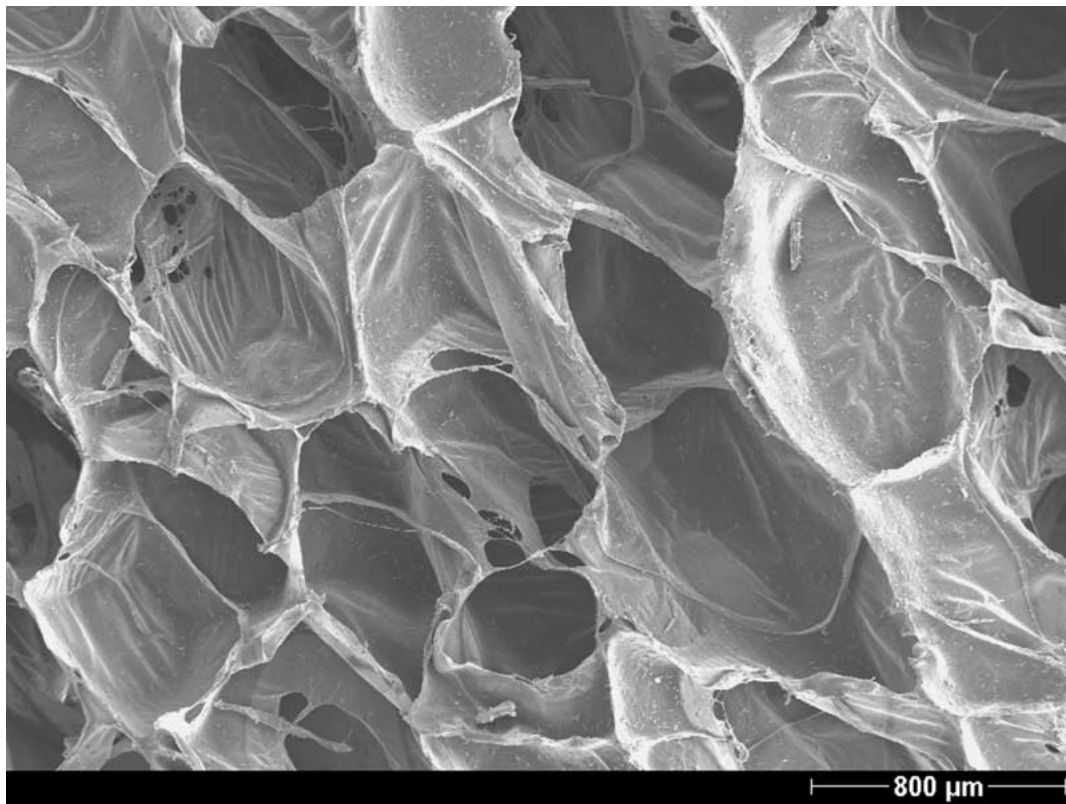
The structural comparison of as-received and transformed foam is shown in Figs 2 and 3. The as received sample of white large cell foam is shown as "a" in Fig. 2. The transformation produced the re-entrant cell morphology. Sample b exhibited negative Poisson's ratio behaviour. Previous studies of polyurethane foams have shown a range of compression ratios that may be used in order to achieve a re-entrant structure and negative Poisson's ratio behaviour. The optimum compression ratio was around 3.5 in that system, but 2.0 was sufficient to achieve a negative Poisson's ratio.

Microcellular foam responded to the transformation by a reduction of the cell size with no evidence of a

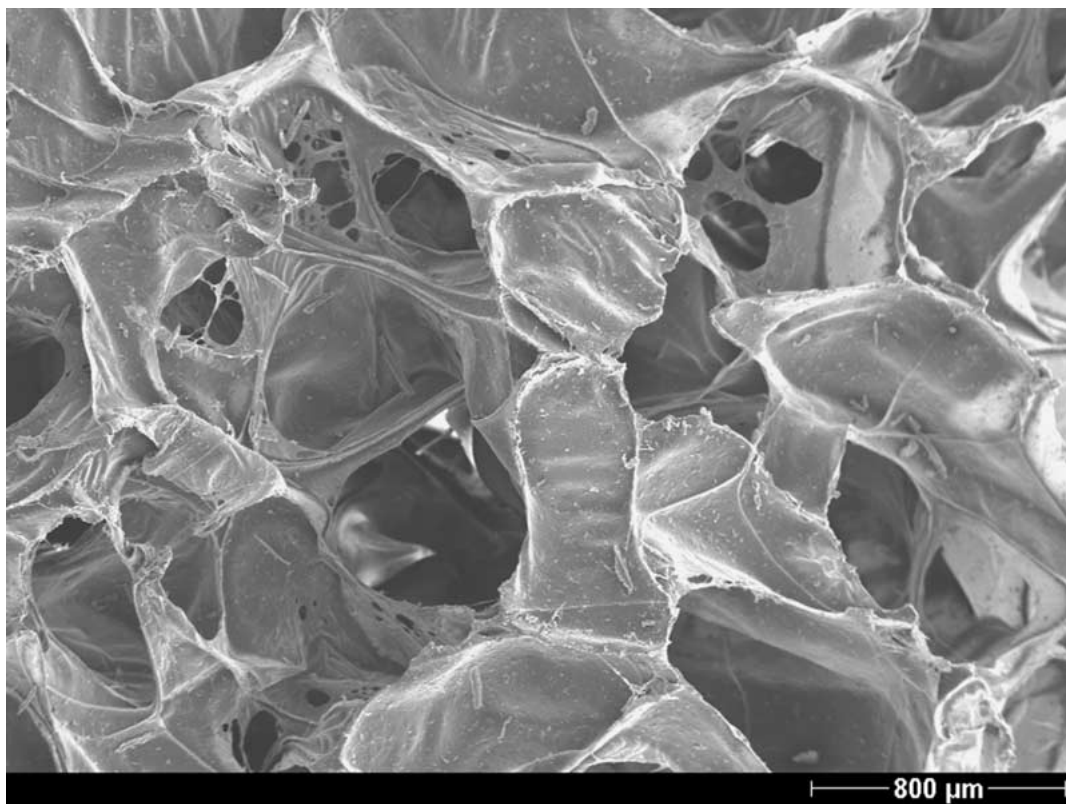
re-entrant structure (Fig. 3). Both transformed samples were processed at 160°C for fourteen minutes and quenched before removal from the mold. Rolling procedures did not break the cell walls; micrographs disclosed the rolled foam remained closed cell.

3.2. DSC and solubility

Differential scanning calorimetry results are shown in Fig. 4. The graph discloses large cell foam to have a softening point in the neighborhood of 80°C and microcellular foam to have a softening point closer to

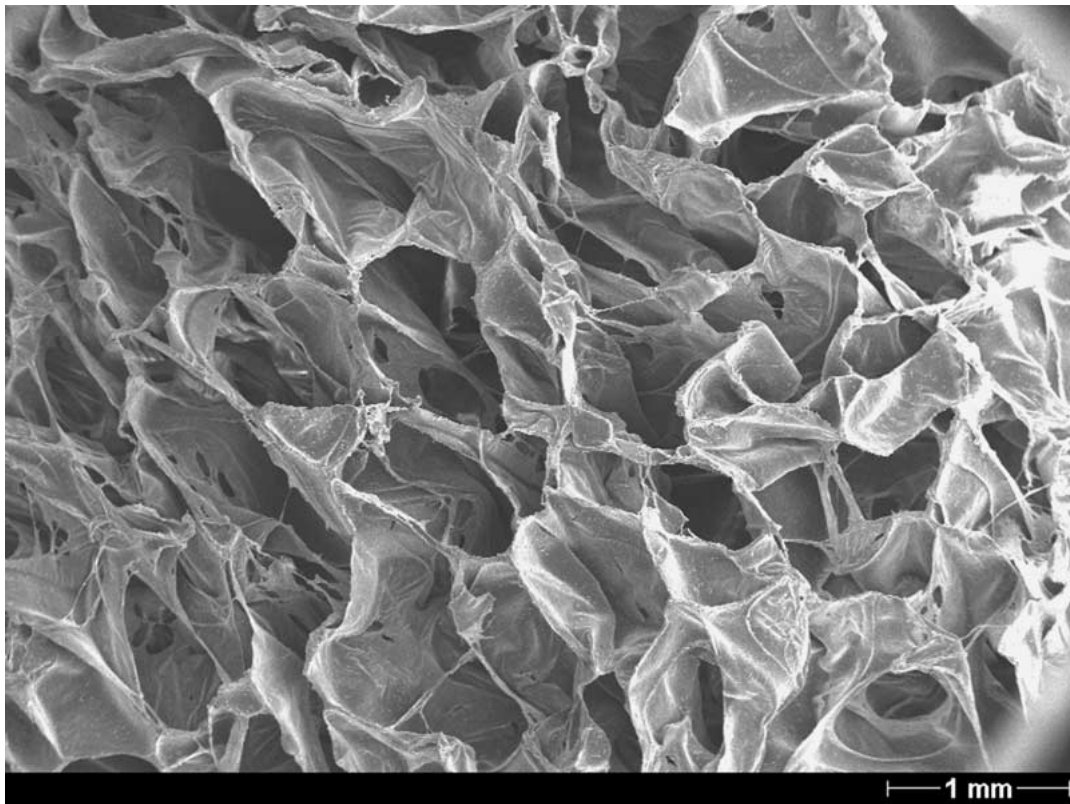


(a)



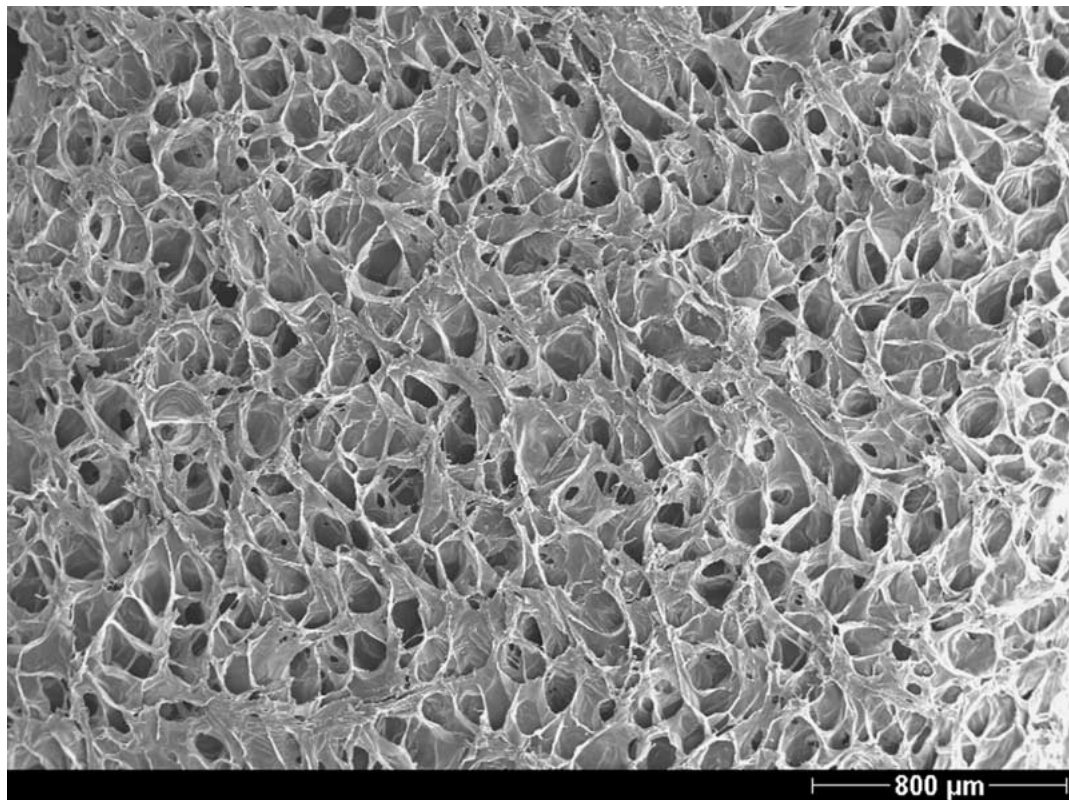
(b)

Figure 2 SEM image of as received and processed white large cell polyethylene foam. Sample a. is as received, sample b. processed with a compression ratio of 2, and sample c. processed with a compression ratio of 3. (Continued)



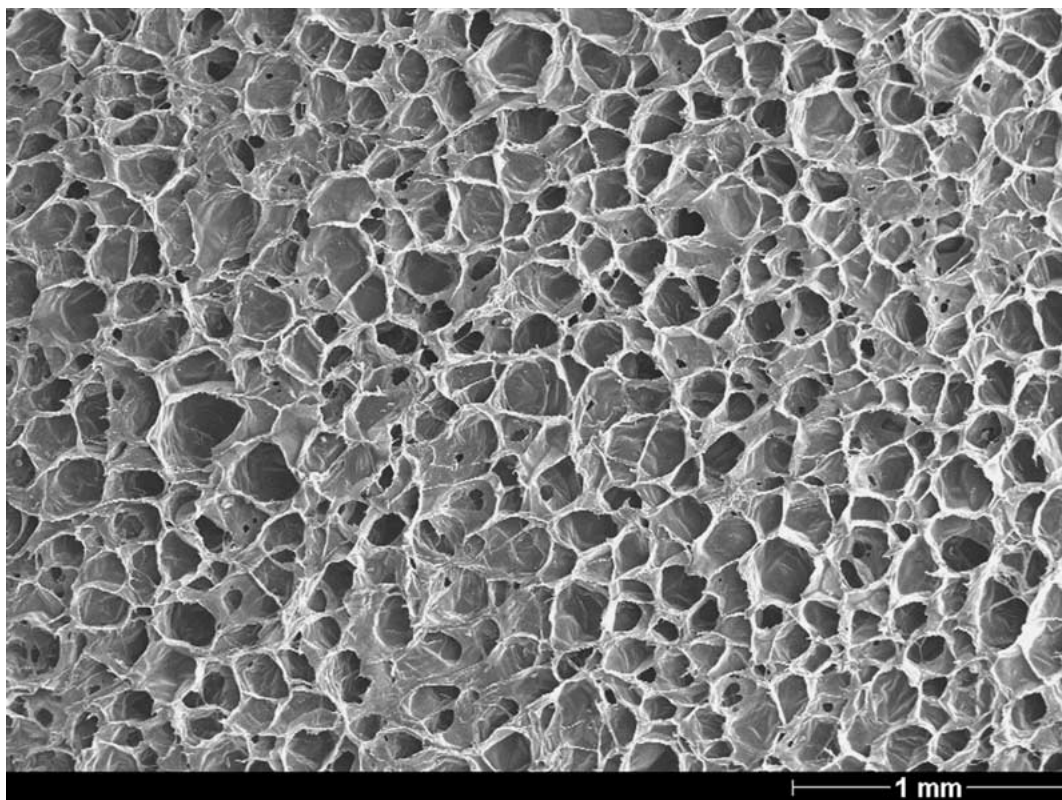
(c)

Figure 2 (Continued).

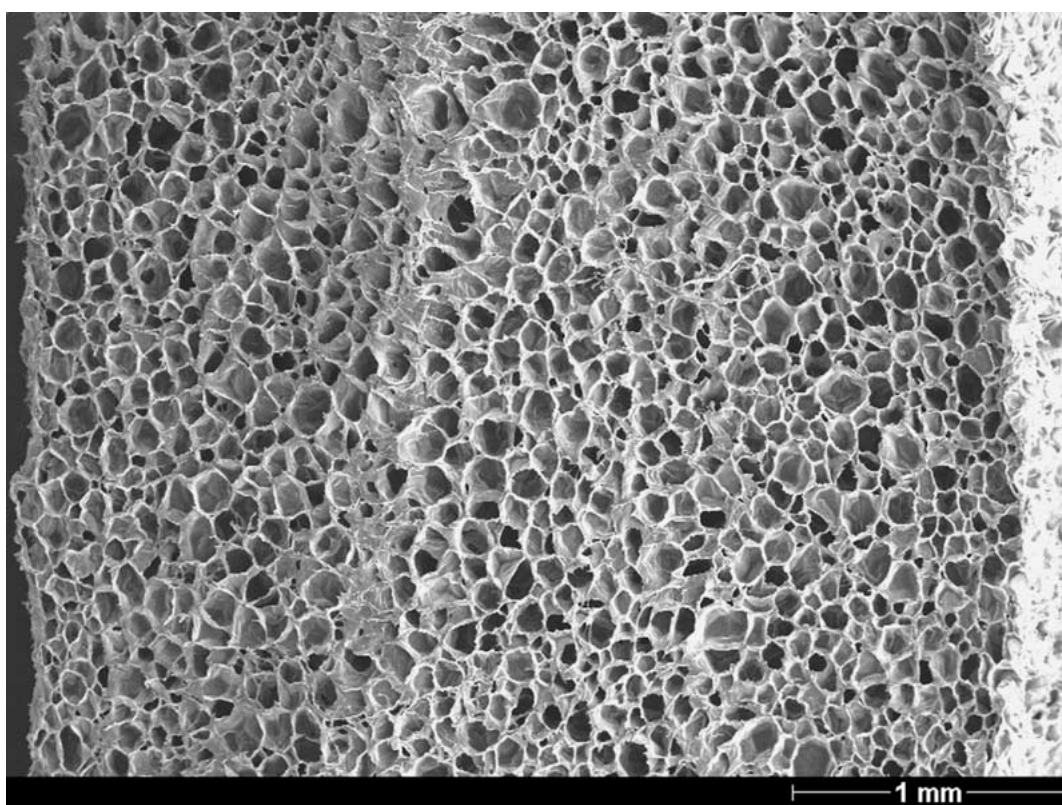


(a)

Figure 3 SEM image of as received and processed microcellular polyethylene foam. Sample a. is as received, sample b. processed with a compression ratio of 2, and sample c. processed with a compression ratio of three. Both sample b and c were processed at 160°C for 14 minutes. (Continued)



(b)



(c)

Figure 3 (Continued).

105°C. This is consistent with our observation that microcellular foam underwent permanent volume change at a higher temperature than required for the large cell material.

Solubility tests showed that none of the three samples could be dissolved in xylene and, therefore, were probably cross-linked polymers.

3.3. Thermal conductivity

The thermal response time constant for a white large cell foam sample with a thickness of 28 mm was about 200 seconds. Microcellular material of the same dimensions resulted in a time constant of 280 seconds. The time constant for foam in a mold was about twice as long, owing to the thermal mass of the mold. These

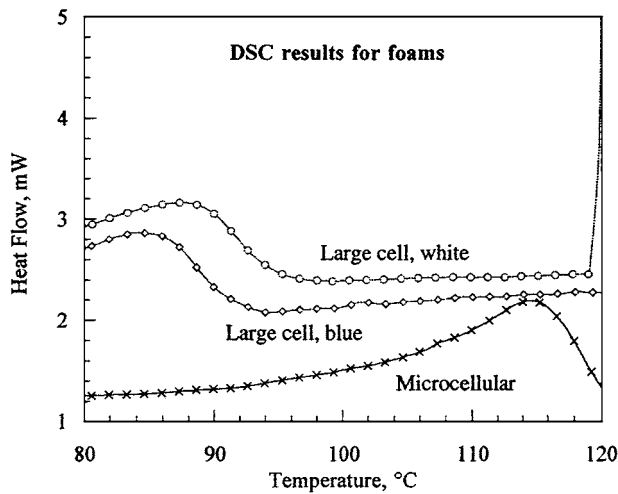


Figure 4 DSC results vs. temperature for several foams.

results provide an idea of how short the processing time can be without gross heterogeneity of transformation.

3.4. Poisson's ratio

3.4.1. Poisson's ratio in relation to processing

Fig. 5 shows the behaviour of the Poisson's ratio in relation to changes in the time and temperature of processing for the blue, large cell foam. A region of minimum Poisson's ratios extends from about 100°C and 12 minutes, through 110°C and eight minutes, to 120°C and five minutes. The time constant due to thermal conductivity of the foam is such that processing for five minutes or less will not transform the entire sample. Samples produced in the regime of high temperature and long time were too soft to remove immediately from the mold. Time and temperature trade-offs were overall similar to those encountered in reticulated polyurethane foam [15], with the difference that polyethylene foam has a lower softening temperature.

For the as-received microcellular foam, Young's modulus in the three orthogonal directions was 1.0 MPa, 1.0 MPa, and 0.97 MPa, suggesting minimal anisotropy. Thermal transformation of microcellular foam gave rise to densification and reduction of cell size rather than rib buckling corresponding to a re-

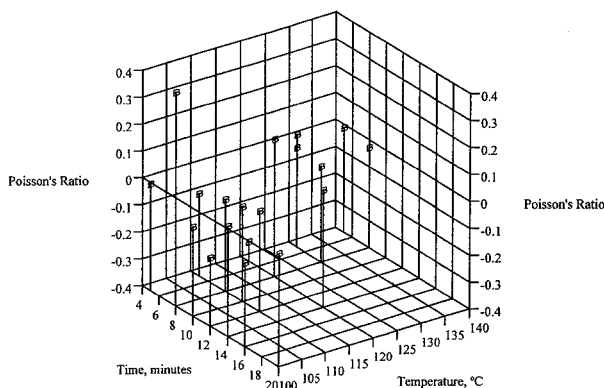


Figure 5 Poisson's ratio vs. processing time and temperature for blue, large cell foam at a compressive strain of 0.15. For the as received material, ν (Poisson's ratio) = 0.03 at this strain.

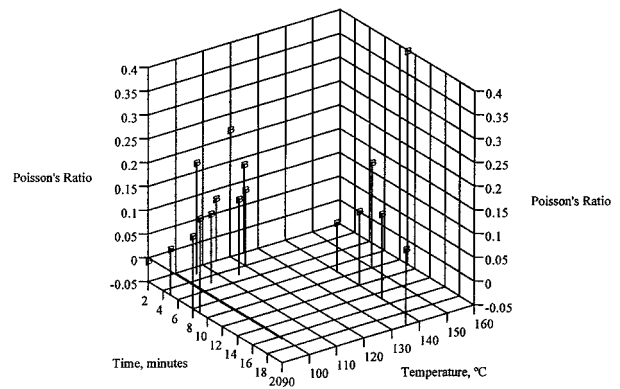


Figure 6 Poisson's ratio vs. processing time and temperature for microcellular foam at a compressive strain of 0.15. For the as received material, $\nu = 0.37$ at this strain.

entrant structure. Substantive negative Poisson's ratio was not observed, as shown in Fig. 6. Rolled microcellular specimens did not exhibit any consistent reductions in Poisson's ratio. Vacuum processed microcellular specimens exhibited a slight decrease in Poisson's ratio, but the value was still positive, about 0.1. Rolled specimens also exhibited positive Poisson's ratio with the exception of one specimen exhibiting a slightly negative value at small strain.

Negative Poisson's ratio has been observed in other porous polyethylene materials. Closed-cell low density polyethylene foam (Ethafoam[®]) was transformed to re-entrant structures with negative Poisson's ratio via hydrostatic air pressure or vacuum treatments [19]. The Ethafoam[®] foams achieved a re-entrant structure after undergoing hydrostatic compression and heat at 621 kPa and 105°C, as well as 621 kPa and 110°C, both for 10 hours, followed by 6 hours of pressure alone. Microporous polyethylene materials with a negative Poisson's ratio were produced by compacting, sintering, and extruding the powdered material [13]. This process differs from the re-entrant transformation process since it does not use foam as a starting material.

Large cell and microcellular polyethylene foams in the present study differ in their transformation characteristics. The difference cannot be attributed to the small cell size alone, since polyurethane foams of cell size 2 mm, 1 mm, and 0.4 mm [13, 15], and 0.25 mm [20] have been transformed successfully. The difference appears not to be related to the closure of cells since all the foams examined here were mostly closed cell. Nevertheless rupture of some cell walls of the large cell foams was audible during the compression process. Moreover, the low density polyethylene foams examined in a prior study [19] were transformed into re-entrant microstructures exhibiting a negative Poisson's ratio. It is likely that a chemical difference is at least partly responsible since a substantial difference in transition temperature was observed in DSC tests. Indeed polyethylene foams [21] differ in the degree of cross linking.

3.4.2. Poisson's ratio vs. strain

All of the as received foams follow the same general trend of decreasing Poisson's ratio with compressive strain as shown in Fig. 7. This effect is attributed to

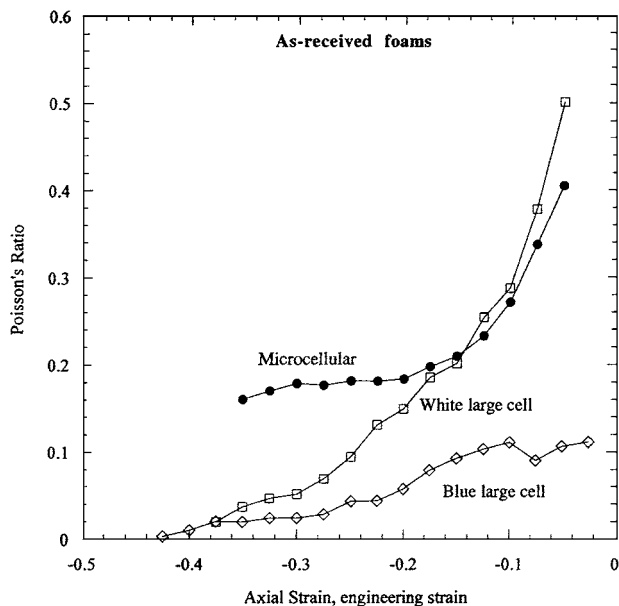


Figure 7 Poisson's ratio vs. compressive axial engineering strain for as-received microcellular, blue, large cell, and white, large cell foams.

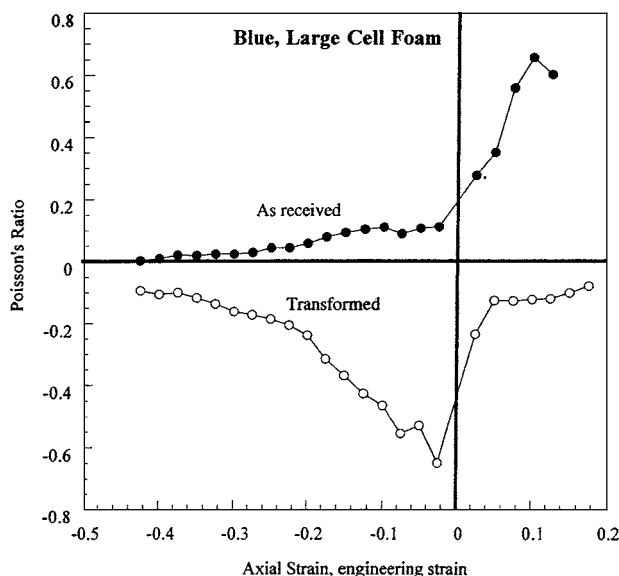


Figure 8 Poisson's ratio vs. axial engineering strain for as received and processed blue, large cell foam. Processing was done at 120°C for 5 minutes with a compression ratio of approximately 2.

the deformation of the cells into a more flattened shape with increasing compressive strain.

Blue, large cell foam in compression and tension, exhibited behaviour as seen in Fig. 8. The Poisson's ratio of the transformed foam reaches a minimum near zero strain and increases in both tension and compression. This is due to the change in angulation of the cell ribs as the structure is stretched or compressed [22, 23]. The nonlinear response of the blue polyethylene foam is similar to that of polyurethane Scott industrial foam [15].

3.4.3. Poisson's ratio vs. time after straining

Poisson's ratio was constant in time over the period 5 sec to 500 sec in a relaxation experiment at con-

stant axial deformation. Although Poisson's ratio in viscoelastic materials can vary with time, no such variation was observed in these studies. Since Poisson's ratio is governed by the geometry of the cells, the cell shape has not changed with time in the relaxation experiment.

4. Conclusions

1. The large cell foams were successfully transformed into materials with re-entrant structure and a negative Poisson's ratio.

2. A region of minimum values of the Poisson's ratio ν was found at an engineering strain of -0.15 for the blue, large cell material. These values ranged from $\nu = -0.14$ to -0.32 under processing conditions ranging from 100°C for 12 minutes to 120°C for 5 minutes, respectively.

3. Poisson's ratio vs. strain in compression and tension for the blue, large cell foam was similar to that of polyurethane samples successfully transformed in the past.

4. Microcellular foam exhibited reduction in cell size with little change in cell shape. Few microcellular samples showed any negative Poisson's ratio behaviour. DSC studies disclosed a shift in transformation temperature in comparison with large cell polyethylene foam, consistent with a difference on the molecular scale.

Acknowledgment

We thank the 3M corporation for their support and encouragement.

References

1. K. C. KHEMANI, in "Polymeric Foams: Science and Technology," edited by K. C. Khemani (American Chemical Society, Washington DC, 1997) p. 1.
2. J. S. COLTON and N. P. SUH, *Polymer Engineering and Science* **27**(7) (1987) 500.
3. M. SHIMBO, D. F. BALDWIN and N. P. SUH, *ibid.* **35** (1995) 1387.
4. V. KUMAR and N. P. SUH, *ibid.* **30** (1990) 1323.
5. V. KUMAR and J. E. WELLER, in "Polymeric Foams: Science and Technology," edited by K. C. Khemani (American Chemical Society, Washington D.C., 1997) p. 101.
6. L. J. GIBSON and M. F. ASHBY, "Cellular Solids: Structure and Properties," 2nd ed. (Cambridge University Press, Cambridge, 1997).
7. C. B. PARK, A. H. BEHRAVESH and R. D. VENTER, in "Polymeric Foams: Science and Technology," edited by K. C. Khemani (American Chemical Society, Washington D.C., 1997) p. 115.
8. P. KANNUS, J. PARKKARI and J. POUTALA, *Bone* **25** (1999) 229.
9. J. G. FLEISCHLI, L. A. LAVERY, S. A. VELA, H. ASHRY and D. C. LAVERY, *Journal of the American Podiatric Medical Association* **87** (1997) 466.
10. Y. C. FUNG, "Foundations of Solid Mechanics" (Prentice-Hall, Englewood, NJ, 1968) p. 353.
11. R. S. LAKES, *Science* **235** (1987) 1038.
12. J. GLIECK, *The New York Times* (14 April 1987).
13. K. L. ALDERSON and K. E. EVANS, *Polymer* **33** (1992) 4435.
14. G. MILTON, *J. Mech. Phys. Solids* **40** (1992) 1105.
15. J. B. CHOI and R. S. LAKES, *J. Mater. Sci.* **27** (1992) 4678.

16. M. GEHLSSEN, 3M corporation, private communication, 1999.
17. H. KUGLER, R. STACER and C. STEIMLE, *Rubber Chemistry and Technology* **63** (1990) 473.
18. C. P. CHEN and R. S. LAKES, *Scripta Metall et Mater.* **29** (1993) 395.
19. E. O. MARTZ, T. LEE, R. S. LAKES, V. K. GOEL and J. B. PARK, *Cellular Polymers* **15** (1996) 229.
20. Y. C. WANG and R. S. LAKES, in preparation.
21. A. MAHAPATRO, N. J. MILLS and G. L. A. SIMS, *Cellular Polymers* **17** (1998) 252.
22. R. S. LAKES, *J. Mater. Sci.* **26** (1991) 2287.
23. J. B. CHOI and R. S. LAKES, *J. Composite Materials* **29** (1995) 113.

*Received 24 July 2000
and accepted 13 July 2001*